Journal of Inclusion Phenomena and Macrocyclic Chemistry (2006) 54:193–200
DOI 10.1007/s10847-005-7367-8

Pseudo[3]rotaxane Type Compelxation between α- and β-Cyc1odextrins and *N*,*N*′-Dsiheptyl-4,4′-bipyridinium

IWAO SUZUKI* and AKIYO YAMAUCHI
Graduate School of Pharmaceutical Sciences, Tohoku University Aramaki, Aoba-ku, 980-8578, Sendai, Japan

(Received: 21 February 2005; in final form: 17 May 2005)

Key words: binding conformation, cyclodextrin, *N*,*N*-diheptyl-4,4-bipyridinium, *p*-nitrophenol, pseudorotaxane, spectral displacement method

Abstract

Pseudo[3]rotaxane type complexation of α- and β-cyclodextrins (α- and β-CDs, respectively) with *N*,*N*′-Diheptyl-4,4′-bipyridinium (diheptyl viologen; HV^{2+}) was investigated. A spectral displacement method using *p*-nitrophenol as a dye revealed that α-CD and HV^{2+} formed a 2:1 host-guest complex with stability constants being 3280 and 976 M^{-1} as the first and second steps of complexation, respectively. ^{1}H-NMR spectra strongly indicated that α-CD accommodated the heptyl groups of HV^{2+}. Although previous studies based on circular dichroism spectroscopy suggested the primary hydroxy side of α-CD faced to the positively charged bipyridinium moiety od HV^{2+}, 2D-NMR studies clearly demonstrated that the secondary hydroxy side of α-CD faced to the bipyridinium moiety. β-CD also formed a 2:1 complex with HV^{2+} with a similar fashion.

Abbreviations: CD– cyclodextrin; cd– circular dichroism; COSY– correlation spectroscopy; HV^{2+}– *N*,*N*′-diheptyl-4,4′-bipyridinium; NOE– nuclear Overhauser effect; NMR– nuclear magnetic resonance; *p*NP– *p*-nitrophenol; ROESY– rotating frame nuclear Overhauser effect spectroscopy; UV– ultraviolet; 1D– one-dimensional; 2D– two-dimensional

Introduction

Rotaxanes and catenanes, which are typical examples of topological chemistry, have been intriguing many chemists' attention. They are now offering us chances to construct nano-meter sized machines [1, 2]. The facile preparation of rotaxanes and catenanes involves the use of host-guest complexation. For this purpose, cyclodextrins (CDs) capable of recognizing alkyl groups [3, 4] has been found as excellent components for rotaxanes, since the Ogino's pioneering study appeared [5], and CD-based rotaxanes and pseudorotaxanes have opened a gate for preparation of organic nano-tubes [6, 7]. Although the vast developments in topological chemistry have realized the construction of molecular-sized nano-machines, limited examples have been reported on the use of rotaxanes and catenanes in molecular recognition chemistry [8, 9]. Rotaxanes and catenanes, however, seem to become excellent hosts in molecular recognition chemistry and chemical sensing. In order to construct sophisticated hosts with excellent guest selectivity as well as efficient signal transduction, it is necessary to assemble several components capable of recognizing parts of guest species, as natural hosts of proteins do. If one can assemble different host components in rotaxanes or catenanes, one can obtain excellent topological chemistry-based host compounds with large size that can recognize large molecules [10]. In this regard, the resulting rotaxanes and catenanes may be regarded as artificial antibodies. In addition, the conformations of rotaxanes and catenanes are expected to be sensitive to external stimuli such as temperature, pH, and guest binding. This must relate to larger changes in spectroscopic signals upon guest binding, leading to excellent chemosensors. In line with this strategy, we initiated our studies on creating rotaxane-based hosts with signal transduction abilities. For the first step of this, we checked the pseudorotaxane formation between α-CD and *N*,*N*′-diheptyl-4,4′-bipyridinum (diheptylviologen, HV^{2+}) in detail, since HV^{2+} has two alkyl groups with suitable length to α-CD complexation on the bipyridinium nucleus. *N*,*N*′-Dialkyl-4,4′-bipyridinium have thoroughly been investigated as excellent components of rotaxanes and catenanes due to their electron deficient nature which results in charge transfer complexation [11–13] and in facile electron transfer to an electrode [14]. In CD chemistry, *N*,*N*′-dialkyl-4,4′-bipyridinium including HV^{2+} have also often been utilized as key components of rotaxanes and catenanes with CDs

* Author for correspondence: E-mail: isuzuki@mail.pharm.tohoku.ac.jp

[15–17]. For α-CD–HV^{2+} system, simple 1:1 complexation has been proposed as a major process, and 2:1 host–guest complexation was neglected [18, 19], despite of the fact that HV^{2+} has two alkyl groups at the opposite ends of the bipyridinium nucleus. Here, we report our findings that HV^{2+} actually binds to α-CD to form a pseudo[3]rotaxane type 2:1 host-guest complex, and that as opposed to the previous report, the secondary hydroxy side of α-CD faces to the bipyridinium moiety. Similar results were obtained for β-CD–HV^{2+} system.

Experimental

General

CDs used in this study were kindly gifted from Yokohama International Bioresearch Co. Ltd. (Yokohama, Japan), and α-CD was used as received. β-CD was recrystallized twice from hot water. CDs were dried *in vacuo* (110 °C, 1 day) prior to use. HV^{2+} was purchased from Tokyo Kasei (Tokyo, Japan), and used as received. *p*-Nitrophenol (*p*NP) was obtained from Wako Pure Chemicals (Osaka, Japan). UV–visible spectra were recorded on a Shimadzu UV-250 spectrophotometer (Kyoto, Japan) with a 1 cm path length quartz cell. Circular dichroism (cd) spectra were taken on a Jasco J-720 spectroporalimeter (Tokyo, Japan). UV–visible and cd spectroscopic measurements were carried out at pH 8.0 borate buffer and at 25.0 °C. ^{1}H-NMR spectra were recorded on a JEOL ECA 600 spectrometer (600 MHz, Tokyo, Japan) at 25.0 °C. D_20 (99.8%-D) was of a product of Isotec (Miamisburg, OH). A residual HDO peak (4.786 ppm) was used as an internal standard [20].

UV–visible measurements and data analyses

To determine the association constants (K) for the complexes of HV^{2+} with CD, a competitive binding method was applied [21]. The proposed equilibria are as follows:

$$HV^{2+} + CD \overset{K_1}{\rightleftharpoons} HV^{2+} : CD \quad (1)$$

$$HV^{2+} : CD + CD \overset{K_2}{\rightleftharpoons} HV^{2+} : CD_2 \quad (2)$$

$$p\mathrm{NP} + CD \overset{K_p}{\rightleftharpoons} p\mathrm{NP} : CD \quad (3)$$

Since the last equilibrium should always be involved as long as *p*NP and CD were present, it was necessary to determine K_p value first. Thus, a buffered aqueous solution (pH 8.0) of *p*NP (4.04×10^{-5} M) was prepared, then a stock solution containing either α-CD (20.0 mM) of β-CD (12.0 mM) were prepared by dissolving CDs with the above *p*NP aqueous solution. Then UV–visible spectrum was recorded for the *p*NP solution (2.500 mL) followed by stepwise addition of the stock solution containing either α-CD or β-CD and *p*NP (1–1000 μL). In this manner, *p*NP concentration was kept at constant. The observed changes of absorbance 407.5 nm for α-CD and at 405 nm for β-CD were analyzed by nonlinear least square regression analyses based on a 1:1 binding model.

To determine K_1, and K_2, a UV–visible spectrum of a buffered aqueous solution (pH 8.0, 2.500 mL) containing 4.04×10^{-5} M of *p*NP and 2.40×10^{-3} M of CD was measured first. Then a solution containing *p*NP (4.04×10^{-5} M), CD (2.40×10^{-3} M), and HV^{2+} (1.00×10^{-2} M) was added stepwise (1–1000 μL) and the UV-visible spectra were recorded at each increment. During the measurements, concentrations of *p*NP and CD were kept constant, while a concentration of HV^{2+} was a variant. The obtained absorbance data were analyzed based on the equilibria (1)–(3). Data analyses were conducted with Microsoft Excel® with SOLVER [22, 23].

Practically, based on a 1:1 binding model for the complexation between CDs and *p*NP, the observed absorbance (A_{obs}) was analyzed with the following equations (Equations (4) and (5)):

$$\begin{aligned} A_{obs} &= \varepsilon_{p\mathrm{NP}} \cdot [p\mathrm{NP}] + \varepsilon_{p\mathrm{NP}-\mathrm{CD}} \cdot [p\mathrm{NP}-\mathrm{CD}] \\ &= \varepsilon_{p\mathrm{NP}} \cdot ([p\mathrm{NP}]_0 - [p\mathrm{NP}-\mathrm{CD}]) \\ &\quad + \varepsilon_{p\mathrm{NP}-\mathrm{CD}} \cdot [p\mathrm{NP}-\mathrm{CD}] \end{aligned} \quad (4)$$

$$[p\mathrm{NP}-\mathrm{CD}] = \frac{K_p([p\mathrm{NP}]_0 + [CD]_0) + 1 - \sqrt{\{K_p \cdot ([p\mathrm{NP}]_0 + [\mathrm{CD}]_0) + 1\}^2 - 4K_p^2[p\mathrm{NP}]_0[\mathrm{CD}]_0}}{2K_p} \quad (5)$$

where ϵ_{pNP} and $\epsilon_{\mathrm{pNP\text{-}CD}}$ denote the molar absorptivities of the free *p*NP and *p*NP-α-CD complex, respectively, and $[p\mathrm{NP}]_0$ and $[\mathrm{CD}]_0$ denote the analytical (initial) concentrations of *p*NP and CD, respectively. The non-linear least-square analyses gave K_p, and $\epsilon_{\mathrm{pNP\text{-}CD}}$ which was an additional unknown parameter. The values of $\epsilon_{\mathrm{pNP\text{-}CD}}$ thus obtained were 2.05×10^4 (407.5 nm) and 1.98×10^4 L mol^{-1} (405 nm) for α-CD and β-CD, respectively, and these values were used for the next step to determine K_1 and K_2 values.

Because of the consideration that the host-guest complexation among HV^{2+}, *p*NP, and CDs involved three complexation phenomena, namely, 1:1 complexation between CDs and *p*NP and 1:1 and 1:2 complexation between HV^{2+} and CD, we applied the following

equations (Equations (6)–(9)) for determining K_1 and K_2. Since only *p*NP and a *p*NP–CD complex show absorptivity at a visible region, and association between *p*NP and HV^{2+} was negligible (*vide infra*), the observed absorbance in the system of HV^{2+}, *p*NP, and CD can still be expressed by Equation (4). However, Equation (5) no longer express the concentration of *p*NP–CD. Instead of Equation (5), we used Equations (6)–(9) for calculating K_1 and K_2 values.

$$K_P = \frac{[pNP - CD]}{[pNP][CD]} \tag{6}$$

$$K_1 = \frac{[HV^{2+} - CD]}{[HV^{2+}][CD]} \tag{7}$$

$$K_2 = \frac{[HV^{2+} - (CD)_2]}{[HV^{2+} - CD][CD]} \tag{8}$$

$$\begin{aligned}[CD] =& [CD]_0 - ([pNP]_0 - [pNP]) \\ & - [HV^{2+} - CD - 2 \cdot ([HV^{2+}]_0 \\ & - [HV^{2+}] - [HV^{2+} - CD])\end{aligned} \tag{9}$$

It is convenient to use SOLVER in Excel® for such a complicated system, because this ad-in program does not require the definition of exact equations expressing $[HV^{2+}]$, $[HV^{2+}-$ CD], [*p*NP], and [*p*NP– CD] which are quadratic equations on $[pNP]_0$, $[CD]_0$, or $[HV^{2+}]_0$. During the calculations, K_1 and K_2 were varied under the restrictions that the concentrations of the every component always satisfied temporal K_1 and K_2 values. A set of K_1 and K_2 values giving the least errors against the experimental absorbance was adopted, finally. At least four independent experiments were performed, and the reported errors were standard deviations on the series of the experiments.

^{1}H-NMR measurements

1D-NMR titration was carried out with a D_2O solution (0.600 mL) of HV^{2+} (2.53 mM). To this solution, an appropriate amount of a D_2O solution containing HV^{2+} (2.53 mM) and CD (10.0 mM) was added stepwise, and ^{1}H-NMR spectra were recorded at each increment. During the titration, HV^{2+} concentration was kept constant. 2D-ROESY spectra were obtained with 1 s of mixing time on HV^{2+} (2.9 mM)–α-CD (4.3 mM) and HV^{2+} (2.6 mM)–*β*-CD (5.0 mM) mixtures. Each spectrum consisted of a matrix of 1 K (Fl) by 1 K (F2) for which zero-filled was applied to making the data sets 2 K by 2 K, and the both dimensions were filtered by a trapezoid 3 window function.

Results and discussion

Stoichiometry and stability of complexes of CDs with HV^{2+}

First, we measured the cd spectrum of HV^{2+} induced by α-CD that provided a chiral cavity for an inserted chromophore. As reported, a broad negative Cotton effect was observed with its trough minimum at 257 nm associated with the absorption band of HV^{2+} [18]. However, the Cotton effect was weak. *β*-CD also induced a Cotton effect at the same region whose intensity was even weaker than that induced by α-CD. As a consequence, we did not pursue to investigate the complexation by cd spectroscopic measurements, and we applied a spectroscopic competitive method to determine the association constants. For this, we first obtained the association constants of CDs with *p*NP (K_p) by UV–visible spectroscopic measurements. Since pK_a of *p*NP is around 6.6, more than 95% of *p*NP is in its anionic form at pH 8.0. *p*NP exhibited a strong absorption band with its peak maximum at 400 nm (data not shown). The addition of α-CD to the solution caused a red-shift of absorption maximum to 407.5 nm with a slight increase in the apparent molar absorptivity, which indicated that α-CD formed a host-guest complex with *p*NP. Definitive isosbestic points at 392 and 442 nm were observed, demonstrating that the stoichiometry of the complex was 1:1. Similarly, the addition of *β*-CD changed the spectrum of *p*NP, although the shift in peak maximum and an increase in the absorbance were less pronounced. The isosbestic point for *p*NP *β*-CD system was found at 393 nm. From the dependence of *p*NP absorption on the CD concentrations, K_p of *p*NP to α- and *β*-CDs were evaluated as 1980 ± 40 and 693 ±

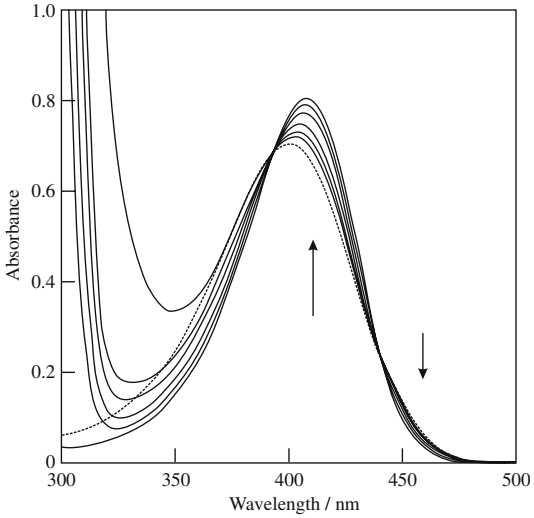

Figure 1. UV–visible absorption spectra of *p*NP (0.0404 mM) in the presence of α-CD (2.40 mM) and varying concentrations of HV^{2+} (0–6.48 mM) in pH 8.0 buffered solutions. The increased absorbance at the shorter wavelength region is due to the HV^{2+} absorption band. The broken line is a UV–visible spectrum of *p*NP alone.

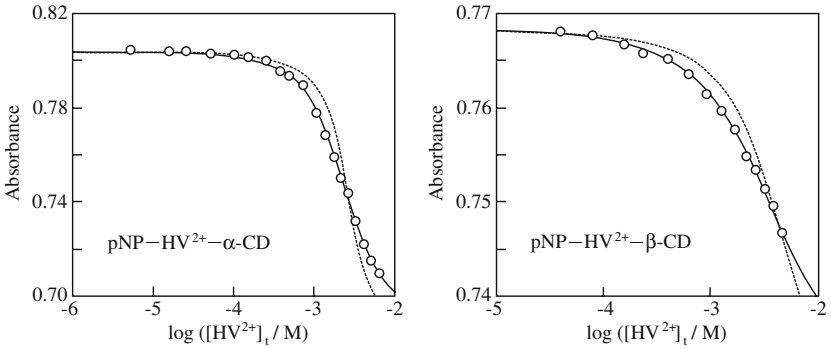

Figure 2. Plots of the absorbance of *p*NP–*β*-CD–HV^{2+} system (left panel; at 407.5 nm) and *p*NP–*β*-CD–HV^{2+} system (right panel; at 405 nm) as a function of HV^{2+} concentration. The solid lines are the best fit biding isotherms considering both 1:1 and 2:1 complex formation between CD and HV^{2+} in addition to 1:1 complex formation between CD and *p*NP. The broken lines are the best fit binding isotherms considering only 1:1 complex formation between CD and HV^{2+} in addition to 1:1 complex formation between CD and *p*NP.

15 M^{-1}, respectively. These values are in good agreement with the reported ones [24, 25].

Figure 1 shows UV–visible spectral changes of *p*NP with α-CD in the presence of HV^{2+}. Since HV^{2+} (and CDs) has no absorption band beyond 350 nm, any absorption bands observed in these spectra are attributed to the *p*NP and *p*NP–CD complexes. Therefore, if HV^{2+} and *p*NP do not interact with each other, observed absorption spectral variations are governed only by the change in molar fractions of *p*NP and *p*NP–CD complex. It is noted that owing to its two positive charges, HV^{2+} can form an ionic complex with negatively charged *p*NP. A relatively high concentration of HV^{2+} (*ca.* 1 mM), however, did never alter the absorption spectrum of *p*NP, which indicated no interaction between *p*NP and HV^{2+}.

As shown in Figure 2, the CD-induced UV–visible absorbance changes of *p*NP fitted well with the theoretical binding isotherm considering both 1:1 and 2:1 host-guest complexation processes with respect to α-CD host and HV^{2+} guest. It is noted that in Figure 1, the isosbestic points still hold, being found at 392 and 442 nm. This strongly supported that the species giving the observed UV–visible absorption spectral changes are only *p*NP and a *p*NP–CD complex. The K_1 and K_2 values for the HV^{2+}–α-CD system obtained from the best-fit curve were 3280 ± 280 and 976 ± 83 M^{-1}, respectively. In the case of *β*-CD, K_1 and K_2 were 338 ± 36 and 536 ± 57 M^{-1}, respectively. The excellent agreement between the experimental data and theoretical binding isotherms confirms the binding model in which HV^{2+} forms both 1:1 and 2:1 host-guest complexes with CDs. We also analyzed experimental data with a model in which CD forms 1:1 host-guest complexes with *p*NP and HV^{2+} independently (omitting the equilibrium (2) in data analyses). The fitting results for this model are also shown in Figure 2 by the dotted lines. We further represent in Figure 3 the result on the system of α-CD–1-heptanol which has only one heptyl group to be accommodated by the α-CD cavity. It is noted that the analysis for α-CD–1-heptanol system is modified a little; the variant in analyses in Figure 2 is the total concentration of HV^{2+}, whereas that in Figure 3 is the total concentration of α-CD. This modification secured the wide concentration range of the variants (HV^{2+} is substantially freely soluble in water, while 1-heptanol has limited solubility to water). From Figure 2, it is obvious that the experimental data were largely deviated from the theoretical binding isotherms based on a 1:1 complexation between CDs and HV^{2+} (Figure 2, dotted lines). In contrast, the α-CD–1-heptanol system (Figure 3) demonstrated excellent agreement between the experimental data and a binding isotherm based on 1:1 complexation between CD and the guest molecule from which an association constant is determined to be 1830 ± 280 M^{-1}. Therefore, we can safely exclude a binding model in which only the 1:1 host–guest complexation between HV^{2+} and α- or *β*-CD is involved.

^{1}H-NMR experiments and complex conformations

^{1}H-NMR titration experiments on HV^{2+}– CD systems were carried out to get insight into the binding conformations. As shown in Figures 4 and 5, marginal shifts were observed for CD protons (3.5–4.0 ppm) in the

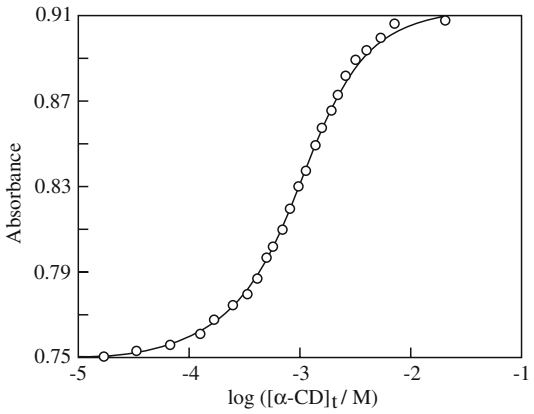

Figure 3. Plots of the absorbance at 407.5 nm as a function of α-CD concentration ([1-heptanol] = 0.672 mM). The solid line is the best fit binding isotherm based on 1:1 complex formation between α-CD and 1-hetanol in addition to 1:1 complex formation between α-CD and *p*NP.

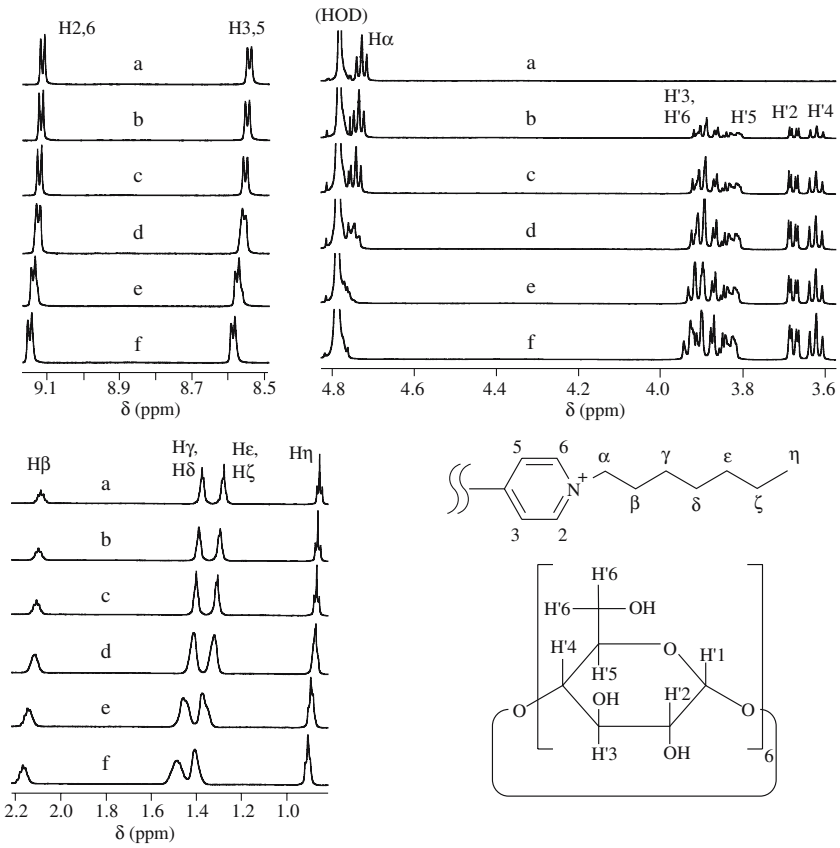

Figure 4. ^{1}H-NMR spectra of α-CD–HV^{2+}; an aromatic region (top left), a CD proton region (top right), and an alkyl region (bottom right) in D_2O. The concentrations of α-CD were 0 (a), 0.42 (b), 0.82 (c), 1.54 (d), 2.75 (e), and 4.55 mM (f), while the HV^{2+} concentration was kept constant (2.53 mM).

presence of HV^{2+}. The signals of uncomplexed and complexed HV^{2+}, α-CD, and *β*-CD were unambiguously assigned on the basis of H–H and C–H COSY results. It is well documented that when CD accommodates an aromatic guest into the cavity, a large (~0.3 ppm or more) upfield shift is observed for H′3 and H′5 protons, which orient towards the interior of a CD cavity [3], due to the magnetic anisotropic effect. Therefore, the titration experiments revealed that the aromatic bipyridinium group of HV^{2+} would not be inserted into the cavities of α- and *β*-CDs. This is in good agreement with the previous report that methylviologen, a methyl analogue of HV^{2+}, did not form any complexes with α- and *β*-CDs [26].

On the other hand, signals assigned to the alkyl groups of HV^{2+} shifted towards a downfield region upon complexation with α-CD; α-CD induced more than 0.13 ppm of downfield shifts for Hγ–Hζ of HV^{2+}, causing substantial broadening on the signals. H*β* and H*η* were also caused downfield shifts, but the magnitude in shifts as well as signal broadening was modest. The observed broadening of the alkyl proton signals implies that the motion of the alkyl groups was restricted by α-CD. The downfield shifts on the alkyl protons would result from the α-CD binding because CD complexation with an alkyl group causes downfield shifts on the accommodated alkyl protons [27]. When the alkyl groups of HV^{2+} are accommodated by α-CD, their motion must be restricted owing to the snug fit between the α-CD cavity and the alkyl groups. This coincides with the observed spectral changes. These ^{1}H-NMR results, thus, strongly indicate that the middle part of the alkyl groups tends to be accommodated by the α-CD cavity.

In contrast to α-CD, *β*-CD affected slightly the signals of alkyl protons of HV^{2+}. However, as noted, no distinct upfield shift was observed for H′3 and H′5 signals of *β*-CD, indicating that the bipyridinium group was not inserted into the *β*-CD. Thus, we consider that *β*-CD also binds to the alkyl groups of HV^{2+}. The smaller downfield shift of the alkyl proton signals may be attributable to the larger cavity size of *β*-CD as well as the smaller association constants of *β*-CD–HV^{2+} complexes. The larger cavity size of *β*-CD may result in the less pronounced signal broadening on the alkyl protons, securing nearly free motion of the accommodated alkyl groups. It is noted that *β*-CD did not cause a downfield shift for H*η* proton signal. This suggests that, as opposed to the α-CD complex, the end part of the alkyl groups of HV^{2+} might not interact with *β*-CD. This was confirmed by 2D-ROESY results as described in the next section.

2D-ROESY experiments gave more straightforward evidences on binding sites of the HV^{2+} in the complexes with CDs [28]. Recently, 2D-ROESY experiments combined with ^{1}H-NMR titration experiments proved multimodal complexation between CDs and a guest

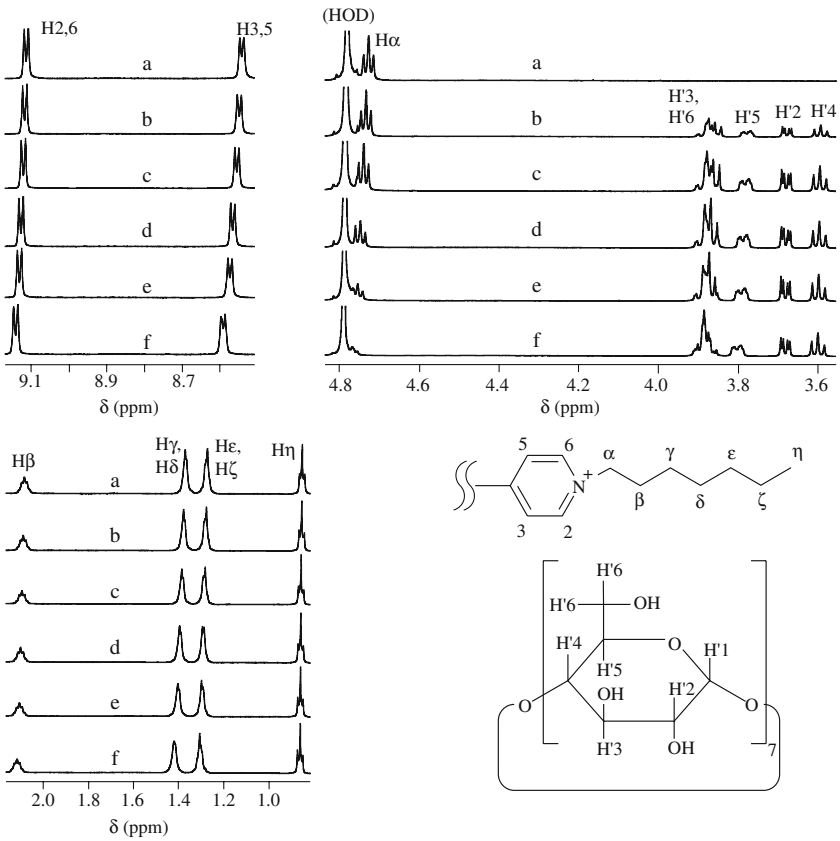

Figure 5. ^{1}H-NMR spectra of β-CD–HV^{2+}; an aromatic region (top left), a CD proton region (top right), and am alkyl regions (bottom right) in D_2O. The concentrations of β-CD were 0 (a), 0.39 (b), 0.75 (c), 1.42 (d), 2.54 (e), and 4.20 mM (f), while the HV^{2+} concentration was kept constant (2.53 mM).

[29–31], and orientational isomerism in CD complexes [32]. As shown in Figure 6, distinct *intermolecular* cross peaks with H′5 were observed for Hϵ to Hη protons, while those with H'3 were observed for Hγ to Hζ protons in the HV^{2+} complex with α-CD. Similarly, as shown in Figure 7, the HV^{2+} complex with β-CD gave *intermolecular* cross peaks for the same region, except for Hη protons. Other protons of HV^{2+} (H2,6, H3,5, Hα, and Hβ) did not give any cross peaks with CD protons, although the aromatic regions was omitted in Figures 6 and 7 for clarity. These results clearly demonstrated that the alkyl groups of HV^{2+} were accommodated into the CD cavities. Moreover, judging from the appearance of the cross peaks for the α-CD complex, the end part of the alkyl group (Hϵ–Hη) was closely located at the H′5 protons at the primary hydroxy side. On the other hand, the observed cross peaks for Hγ (Hδ) protons with H′3 protons indicate that the middle part of the alkyl groups were located at the secondary hydroxy side of CDs.

Based on these results, we proposed the conformations of the complexes of CDs with HV^{2+} as shown in Figure 8. According to the theoretical calculations on cd spectra of CD–chromophore complexes [33], the conformations depicted in Figure 8 might show markedly small cd because the distance from the CD center to the HV^{2+} center are larger than 1.0 nm and because the transition dipole moment of HV^{2+} is parallel to the CD axis. As mentioned above, CD–HV^{2+} complexes showed the weak negative Cotton effects around 257 nm.

The theoretical calculations also suggest that when the chromophore is located just outside the secondary hydroxy side of a CD cavity with its transition dipole moment being parallel to the CD axis, the sign of the Cotton effect is positive. However, the sign may be inverted if the distance between centers of the chromophore and CD is longer than 1.0 nm. This would be the case of CD–HV^{2+} complexes investigated here.

The orientation of CDs proposed as Figure 8 is reasonable for CD–HV^{2+} complexes, especially for α-CD complexes, because α-CD has an electrostatic potential gradient by which the primary hydroxy side is positively polarized [34]. The positively charged bipyridinium group, thus, tends to exist at the secondary hydroxy side to minimize the electrostatic repulsion. The potential gradient of α-CD was larger than that of β-CD. This may cause the difference in appearance of NOEs in the 2D-ROESY results and in the downfield shift patterns in the ^{1}H-NMR titration results between α-CD and β-CD. The larger potential gradient of α-CD strongly prohibits the bipyridinium group from approaching to the α-CD cavity. This results in the accommodation of Hη protons by the α-CD cavity to experience the large downfield shift in ^{1}H-NMR titration and to exhibit NOE signals with H′5 protons. On

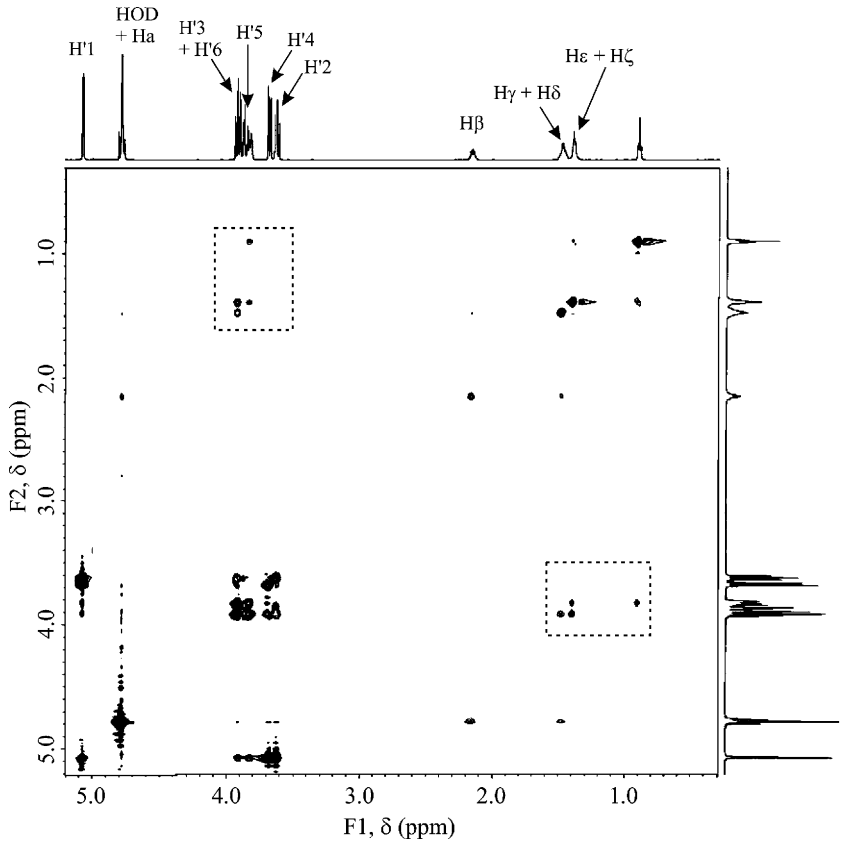

Figure 6. 2D-ROESY plots of α-CD (4.3 mM) – HV^{2+} (2.9 mM) measured in D_2O. Cross peaks appearing in the dashed square are *intermolecular* NOEs. Under the experimental conditions, the molar fractions of 2:1 complex, 1:1 complex, and free HV^{2+} were 0.37, 0.45, and 0.18, respectively,

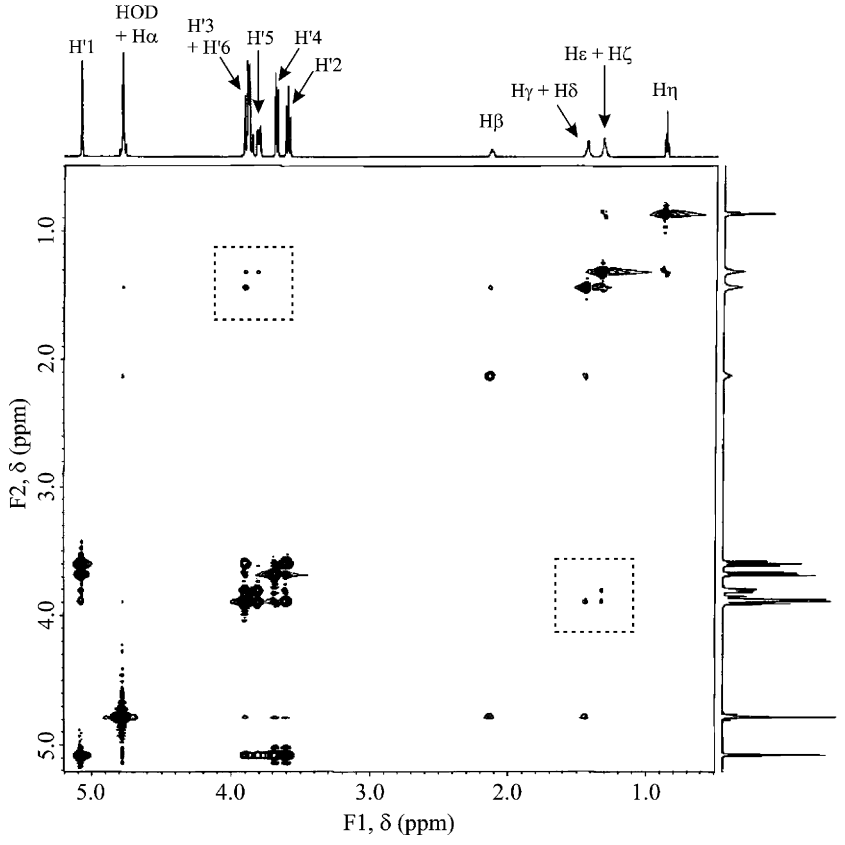

Figure 7. 2D-ROESY plots of β-CD (5.0 mM) – HV^{2+} (2.6 mM) measured in D_2O. Cross peaks appearing in the dashed square are *intermolecular* NOEs. Under the experimental conditions, the molar fractions of 2:1 complex, 1:1 complex, and free HV^{2+} were 0.36, 0.29, and 0.35, respectively.

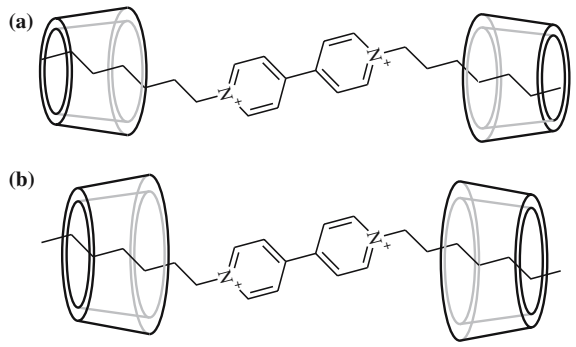

Figure 8. Schematic illustration of a proposed structures for 2:1 complexes of HV^{2+} with (a) α-CD and (b) β-CD.

the other hand, the facts that no shift in Hη at protons and no NOE signals between Hη protons and β-CD protons were observed clearly demonstrate that the Hη protons are never accommodated into the β-CD cavity. This difference is also illustrated in Figure 8.

It is noteworthy that our findings that the secondary hydroxy side of CDs oriented towards the HV^{2+} when they accommodated the alkyl groups of HV^{2+} may give important information to construct more sophisticated CD-based synthetic receptors, because one of the hot topics in CD chemistry is to control guest selectivity and orientational isomerism of an included guest [35].

Conclusion

Both α- and β-CDs formed 2:1 host-guest complexes together with 1:1 complexes with HV^{2+}, forming pseudo[3]rotaxanes. ^{1}H-NMR studies revealed that the alkyl groups of HV^{2+} were binding sites to CDs. In the complexes, the secondary hydroxy sides of CDs were faced to the bipyridinium group of HV^{2+}. These conclusions are somewhat different from previously reported conclusions derived from the sign of cd spectrum that α-CD formed 1:1 a complex with HV^{2+} with the primary hydroxy side being located near the bipyridinium group [16]. Based on the results obtained here, we have initiated to construct pseudorotaxanes and rotaxanes in which modified CDs having a molecular recognition part at the rim of CD cavities are involved as wheels of rotaxanes to create novel receptors not only for inorganic but also for organic guests with signal transduction abilities. Besides, the electron deficient nature of HV^{2+} may offer us a chance to use an old, but less utilized charge-transfer complex formation in supramolecular chemosensors. According to this idea, exploration of complexation phenomena between HV^{2+} with CD derivatives with electron rich pendants is also underway.

Acknowledgments

This work was financially supported by a Grant-in-Aid for Scientific Research (15659006 and 16790030) from Japan Society for Promotion of Science, and by the Shorai Foundation. One of the authors (A. Y.) is also grateful to the Toray Scientific Foundation for financial support in part. We would like to appreciate Dr. Yoshiyuki Tanaka of our Graduate School for his valuable help to the data analyses.

References

1. V. Balzani, A. Credi, F. Raymo, and J.F. Stoddart: *Angew. Chem. Int. Ed.* **39**, 3378 (2000).
2. S.J. Rowan, S.J Cantrill, G.R.L. Cousins, J.K.M. Sanders, and J.F. Stoddart: *Angew. Chem. Int. Ed.* **41**, 898 (2002).
3. M.L. Bender and M. Komiyama: *Cyclodextrin Chemistry*, Springer, New York (1978).
4. J. Szejtli and T. Osa (eds.): *Cyclodextrins (Comprehensive Supramolecular Chemistry Vol 3)*, Pergamon, Oxford (1996).
5. H. Ogino: *J. Am. Chem. Soc.* **103**, 1303 (1981).
6. Harada: *Nature (London)* **356**, 325 (1992).
7. A. Harada, J. Li, and M. Kamachi: *Nature (London)* **364**, 516 (1993).
8. I. Smukste, B.E. House, and D.B. Smithrud: *J. Org. Chem.* **68**, 2559 (2003).
9. V. Dvornikovs, B.E. House, M. Kaetzel, J.R. Dedman, and D.B Smithrud: *J. Am. Chem. Soc.* **125**, 8290 (2003).
10. A. Nelson, J.M. Belitsky, S. Vidal, C.S. Joiner, L.G. Baum, and J.F. Stoddart: *J. Am. Chem. Soc.* **126**, 11914 (2004).
11. A.R. Bernardo, J.F. Stoddart, and A.E. Kaifer: *J. Am, Chem. Soc.* **114**, 10624 (1992).
12. P.E. Mason, I. Parsons, and M.S. Tolley: *Angew. Chem. Int. Ed. Engl.* **35**, 2238 (1996).
13. E. O. Katz Lioubashevsky and I. Willner: *J. Am, Chem. Soc.* **126**, 15520 (2004).
14. T. Lu, L. Zhang, G.W. Gokel, and A.E. Kaifer: *J. Am, Chem. Soc.* **115**, 2542 (1993).
15. C. Lee, M. Sung, S. Moon, and J.-W. Park: *J. Electroanal. Chem.* **407**, 161 (1996).
16. J. Woon, B.-A. Lee, and S.-Y. Lee: *J. Phys. Chem. B* **102**, 8209 (1998).
17. Y. Kawaguchi and A. Harada: *Org. Lett.* **2**, 1353 (2000).
18. M. Kodaka and T. Fukaya: *Bull. Chem. Soc. Jpn.* **59**, 2032 (1986).
19. M. Kodaka and T. Fukaya: *Bull. Chem, Soc. Jpn.* **62**, 1154 (1989).
20. N. Funasaki, S. Ishikawa, and S. Neya: *Bull. Chem. Soc. Jpn.* **75**, 719 (2002).
21. L.A. Selvidge and M.R. Eftink: *Anal. Biochem.* **154**, 400 (1986).
22. K. Hirose: *J. Inclusion Phenom. Macrocycl. Chem.* **39**, 193 (2001).
23. D.C. Harris: *Chem. Edu.* **75**, 119 (1998).
24. G.L. Bertrand, J.R. Faulkner, S.M. Han, and D.W. Armstrong: *J. Phys. Chem.* **93**, 6863 (1989).
25. R.J. Bergeron, D.M. Pillor, G. Gibeily, and W.P. Roberts: *Bioorg. Chem.* **7**, 263 (1978).
26. T. Matsue, T. Kato, U. Akiba, and T. Osa: *Chem. Lett.,* 1825 (1985).
27. N. Funasaki, S. Ishikawa, and S. Neya: *J. Phys. Chem. B* **107**, 10094 (2003).
28. H.-J. Schneider, F. Hacket, V. Rildiger, and H. Ikeda: *Chem. Rev.*, 1755 (1998).
29. A. Jover, R.M. Budal, F. Mejide, V.H. Soto, and J.V. Tato: *J. Phys. Chem. B* **108**, 18850 (2004).
30. C.M. Fernandes, R.A. Carvalho, S.P. Costade, and F.J.B. Veiga: *Eur J. Pharm. Sci.* **18**, 285 (2003).
31. M. Miyauchi and A. Harada: *J. Am. Chem. Soc.* **126**, 11418 (2004).
32. H. Yamamura, M.V. Rekharsky, Y. Ishihara, M. Kawai, and Y. Inoue: *J. Am. Chem. Soc.* **126**, 14224 (2004).
33. M. Kodaka: *J. Phys. Chem.* **95**, 21102112.
34. M. Sakurai, M. Kitagawa, H. Hoshi, Y. Inoue, and R. Chûjô: *Chem. Lett.,* 895 (1988).
35. A. Nakamura and Y. Inoue: *J. Am. Chem. Soc.* **127**, 5338 (2005).